Physics of the Solid State, Vol. 43, No. 4, 2001, pp. 644–651. Translated from Fizika Tverdogo Tela, Vol. 43, No. 4, 2001, pp. 619–626.

SEMICONDUCTORS AND DIELECTRICS

Dispersive Characteristics of Diamond in the Range of Hard X-ray Waves

A. G. Tour'yanskiĭ, I. V. Pirshin, R. A. Khmel'nitskiĭ, and A. A. Gippius

Lebedev Physical Institute, Leninskiĭ pr. 53, Moscow, 117924 Russia

e-mail: tour@sci.lebedev.ru

Received July 6, 2000; in final form, August 17, 2000

Abstract—Dispersive properties of natural diamonds were studied for the first time in a range of x-ray wavelengths of 0.03–0.2 nm. The dispersion element represented an analog of a rectangular prism. A collimated beam of polychromatic radiation was directed onto the refracting face from inside under a small glancing angle ($\ll\pi/2$). The radiation was introduced into the prism through a side face oriented perpendicularly to the axis of the incident beam. In the range of energies near 8 keV, a resolution of 106 eV was achieved, which is about twice as good as the corresponding parameter for semiconductor detectors. Calculations show that under ideal conditions the limiting resolution for a diamond prism with a single refracting face can be reduced to 36–40 eV. This makes it possible to create a new type of analytical devices—dispersion x-ray spectrometers for the investigation of rapid processes involving generation and absorption of x-ray radiation. © *2001 MAIK "Nauka/Interperiodica".*

INTRODUCTION

For a detailed analysis of spectra of x-ray radiation propagating in a given direction in the range of $\lambda <$ 0.3 nm, monochromators made of perfect single crystals are used as a rule [1, 2]. For a fixed orientation of the unit vector $\mathbf{S}_0$ that characterizes the specified direction, reflection can occur only in narrow spectral intervals in accordance with the Bragg condition for diffraction. Therefore, in order to investigate the total spectrum in a wide spectral range, it is necessary to mechanically rotate the monochromator and multiply repeat measurements. It is obvious that such a method is inapplicable for the investigation of nonstationary fast processes, e.g., those occurring upon irradiation of a target with a power laser pulse [3]. Note that in practice the spectrum of the radiation that is reflected from a crystal monochromator is frequently detected using a photographic plate or other types of two-dimensional position detectors [4]. However, the condition of the constancy of $\mathbf{S}_0$ is violated in this case.

Pulsed radiation spectra also cannot be studied using cooled semiconductor detectors [5], since a fundamental condition for them to operate is a successive registration of isolated quanta in time intervals of $\geq$10 μs [6]. Diffraction gratings, which are widely used in the optical and soft x-ray spectral ranges, possess a low efficiency (~1%) at wavelengths less than 0.3 nm [7, 8]. In addition, uncontrolled distortions caused by the strong anisotropy of scattering are superimposed onto the spectrogram, since in the case of artificial periodic structures the radiation wavelength λ is much smaller than the grating period p.

Thus, at present, there is likely to be no suitable experimental means for the spectrometry of directional polychromatic beams of hard x-ray radiation generated during fast nonstationary processes.

In this work, we show for the first time that the dispersive properties of diamonds make it possible to decompose spectra of hard x-ray radiation with wavelengths down to 0.03 nm (E = 40 keV) and, owing to angular dispersion, to analyze the spectra of both stationary and pulsed sources without any limitations on the pulse duration.

1. EXPERIMENTAL

Figure 1 displays a schematic of an experimental setup we designed to perform dispersion measure-

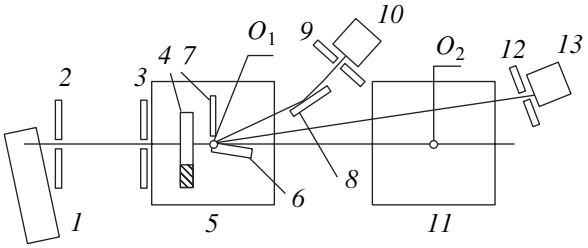

Fig. 1. Schematic of the experimental setup for measuring dispersion: (*1*) x-ray tube; (*2*, *3*, *9*, *12*) vertical collimating slits; (*4*) movable horizontal slit; (*5*, *11*) goniometers; (*6*) sample; (*7*) protecting absorbing shield; (*8*) monochromator; and (*10*, *13*) radiation detectors.

1063-7834/01/4304-0644$21.00 © 2001 MAIK "Nauka/Interperiodica"

ments. The source of radiation is a sharp-focus x-ray tube with a copper anode. The visible dimension of its focus in the measurement plane is 40 μm. Along the x-ray beam, two x-ray goniometers are mounted. The distances from the focus of the x-ray tube to the main axes O_1 and O_2 of goniometers *5* and *11* are 330 and 1161 mm, respectively, and those from the axes O_1 and O_2 to the entrance slits *9* and *12* are 225 and 192 mm, respectively. With an entrance slit of 30 μm wide, this scheme ensures an angular resolution of 0.0076° for the first (along the beam) goniometer *5* and 0.0017° for goniometer *11*.

As the samples, we used crystals of natural diamond (type Ia) with a density of 3.515 g/cm^3. The base (refracting) face was parallel to the (110) plane; perpendicularly to this base, two parallel side faces were prepared by lapping and polishing. The polishing of the surfaces was performed using an ASM28/20 diamond powder. The refracting face was additionally polished using a finer powder with an average grain size of ~1 μm. Three samples were prepared. The dimension of the refracting face (which has a minimum area of 12 mm^2) in the incidence plane of the beam was 2.2 mm. For comparison, we also used a single-crystal silicon plate cut from a standard optically polished wafer. In this case, the side surfaces perpendicular to the base face were obtained by cleaving on silicon cleavage planes.

The samples were mounted in such a manner that the edge formed by the base and the side surface facing the focus of the x-ray tube be coincident with the rotation axis O_1 of goniometer *5* (Figs. 1, 2). The typical angular divergence of the beam incident on the refracting face of the dispersive element was 24″. A graphite monochromator *8* and detector *10* mounted on a rotary arm were used to preliminarily adjust the x-ray scheme. All the results that are given below were obtained by angular scanning using detector *13* with an NaI(Tl) scintillator crystal with rotation about the O_2 axis. The program of controlling the data acquisition at a constant velocity of the detector made it possible to use an arbitrary time of data acquisition at each angular position. A typical angular interval between the readings was 0.0005°.

2. ANGULAR DISPERSION UPON REFRACTION OF X-RAYS

Let us consider (in terms of geometric optics) the passage of a parallel x-ray beam through a rectangular prism of a uniform material. We designate the refractive indices of the prism and the ambient medium $n_1(\lambda) = 1 - \delta_1(\lambda) - i\beta_1(\lambda)$ and $n_2(\lambda) = 1 - \delta_2(\lambda) - i\beta_2(\lambda)$, respectively. Let the *z* axis be perpendicular to and the *x* axis be parallel to the first interface and let them lie in the incidence plane (Fig. 2). Let the radiation be monochromatic ($\lambda \sim 0.1$ nm) and the angle φ of incidence onto the first interface be close to zero. Under the above

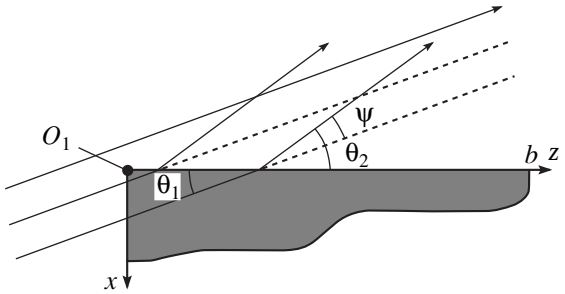

Fig. 2. Geometry of the x-ray radiation path for the case where a beam to be analyzed strikes from inside the refracting surface of a diamond crystal.

conditions, the following simplifications are possible. First, we can consider only refraction at the second interface, since the magnitudes of the coefficient of reflection and the changes in the refraction angle upon the intersection of the first interface are negligibly small. Second, we can ignore the state of polarization of the incident radiation, since, according to the Fresnel formulas, the coefficients of transmission for the *s* and *p* polarizations are virtually coincident at $\varphi \longrightarrow \pi/2$. Going from incidence angles φ to glancing angles $\theta = \pi/2 - \varphi$, we can transform the sine law [9] for the second interface to the form

$$\frac{1 - \delta_1 - i\beta_1}{1 - \delta_2 - i\beta_2} = \frac{\sqrt{1 - \sin^2\theta_2}}{\sqrt{1 - \sin^2\theta_1}}, \qquad (1)$$

where θ_1 and θ_2 are the glancing angles for the incident and refracted radiations in the first and second media, respectively. The absolute magnitude of the decrement of the refractive index $|\delta + i\beta|$ for the wavelength used is less than 10^{-4} [10] ($\beta/\delta \ll 1$). This circumstance permits us to use, in the range of small glancing angles ($\theta_1 \ll \pi/2$), the expansion into a series and obtain the following expression for the glancing angle θ_2 of the refracted radiation in the second medium:

$$\theta_2 \cong \sqrt{\theta_1^2 - 2(\delta_2 - \delta_1)}. \qquad (2)$$

Let us differentiate Eq. (2) with respect to θ_1. Then, for a beam with an angular divergence $\Delta\theta$, we obtain the following dependence of the coefficient of angular contraction C_a on θ_1 (here, θ_1 is the glancing angle of the central beam):

$$C_a = \frac{\Delta\theta_1}{\Delta\theta_2} = \frac{\sqrt{\theta_1^2 - 2(\delta_2 - \delta_1)}}{\theta_1}. \qquad (3)$$

The decrement of the refraction index of air δ_2 can be neglected. As follows from Eq. (3), in the geometry that was chosen (Fig. 2), there occurs an angular contraction of the refracted beam ($C_a > 1$). Note that upon the reversion of the beam direction, i.e., upon the passage of the

radiation from air into the sample, the angular cone of the refracted beam will increase, since in this case $C_a < 1$. Consequently, in our case, a maximum angular resolution of the spectrum is observed.

Now, we take into account the spectral dependence of the refractive index. In the spectral range under consideration, the condition $\nu_0^2 \gg \nu_i^2$ for all electron shells of the C atom is fulfilled (here, ν_0 is the frequency of vibrations corresponding to an arbitrary line in the x-ray range under study and ν_i is the natural frequency of vibrations of an electron of the *i*th shell). Under the above condition, in accordance with the electron theory of dispersion [10], we have for any line λ of the x-ray spectrum

$$\delta\lambda = g\rho\lambda^2, \tag{4}$$

where g is a dimensional coefficient (which can be expressed through fundamental physical constants) and ρ is the physical density of the sample. Substituting Eq. (4) into Eq. (2) and differentiating with respect to λ, we obtain the following expression for the angular dispersion:

$$D(\rho, \lambda) = d\theta_2/d\lambda = \frac{2\lambda g\rho}{\sqrt{\theta_1^2 - 2g\rho\lambda^2}}. \tag{5}$$

It is obvious that at grazing angles ($\theta_1 \longrightarrow 0$) the angular dispersion is maximum. In this case, $D \propto \rho^{1/2}$ and is independent of λ. At $\theta_1^2 \gg 2g\rho\lambda^2$, the magnitude of $D(\rho, \lambda)$ changes approximately proportionally to ρ and λ. As is known from the theory of prism spectrometers [11], the spectral resolution $A = \lambda/\Delta\lambda$ is related to the diffraction limit. In the case under consideration, the effective cross section of the refracted beam in the plane of incidence can be restricted by two factors: first, the finite size of the elemental refracting area b and, second, the finite mean free path of photons in the sample, which is equal to the inverse linear coefficient of absorption $\mu(\lambda)$. More strictly, we can write the following expression for the diffraction angular width $\Delta\theta(\lambda)$ of the refracted beam:

$$\Delta\theta_d\lambda \cong \begin{cases} \lambda/b\theta_2, & b \le 2/\mu(\lambda) \\ \lambda\mu(\lambda)/2\theta_2, & b \ge 2/\mu(\lambda). \end{cases} \tag{6}$$

The introduction of the factor 2 is caused by the fact that, when estimating the diffraction broadening, we should take into account a decrease in the wave amplitude. For the regions of the x-ray spectrum near the CuK_α (0.154 nm) and CuK_β (0.139 nm) characteristic lines, the condition $b \ge 2/\mu(\lambda)$ is fulfilled. Substituting into Eq. (6) the value of $\mu(\lambda)$ for diamonds for the above-indicated wavelengths and the typical value of the angle $\theta_2 = 0.2°$ (3.5 mrad), we obtain $\Delta\theta_d(\text{Cu}K_\alpha) \approx 0.0019°$ (32 mrad) and $\Delta\theta_d(\text{Cu}K_\alpha) \approx 0.0012°$ (2.1 mrad). This permits us to estimate the spectral resolution $A(\lambda)$ of the dispersive element. Multiplying the left-hand and right-hand parts of Eq. (5) by $\Delta\lambda$ and substituting the values of the constants corresponding to the indicated parameters, we find $A_\alpha = 200$ and $A_\beta = 251$. By going from $\Delta\lambda$ to the energy resolution, we obtain $\Delta E = 40$ and 36 eV for the lines with the wavelengths 0.154 and 0.139 nm, respectively.

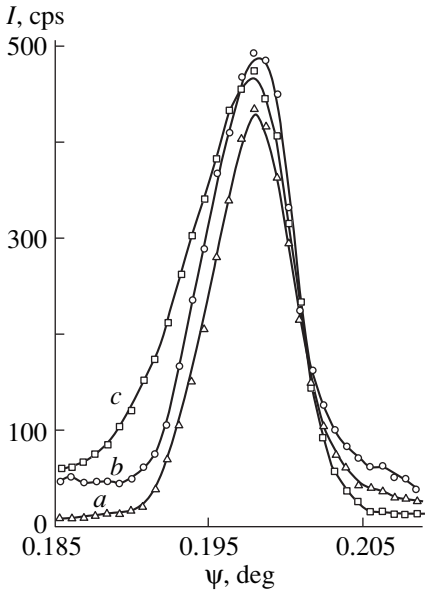

Fig. 3. Angular profiles of the refracted beam for the CuK_α line for three diamond samples (*a*–*c*). The beam strikes the refracting surface from inside the sample; the fixed glancing angle is $\theta_1 = 0.09°$.

3. MEASUREMENT RESULTS

Figure 3 displays the angular profiles of the refracted beam for three diamond samples (*a*, *b*, and *c*) measured under identical irradiation conditions. Hereafter, the abscissa axis corresponds to the deviation angle $\varphi = \theta_2 - \theta_1$ measured from the direction of the primary beam. The beam analyzed passed, in accordance with the geometry of the scheme shown in Fig. 2, through the side face and fell from inside on the base surface of the sample. The maintenance of a constant magnitude of the glancing angle θ_1 is a fundamental condition for obtaining maximum resolution. As can be seen from the comparison, the width at the half-height of the refraction peak is minimum for sample *a*. This indicates that the major part of its refracting surface meets the condition of maximum planeness. Therefore, we used just this sample for further measurements.

With decreasing glancing angle θ_1, the angular dispersion should increase according to Eq. (5). As was shown in [12], the effective width of the entrance aperture of a dispersion element for the spectral line with a wavelength λ in the geometry of Fig. 2 is equal to

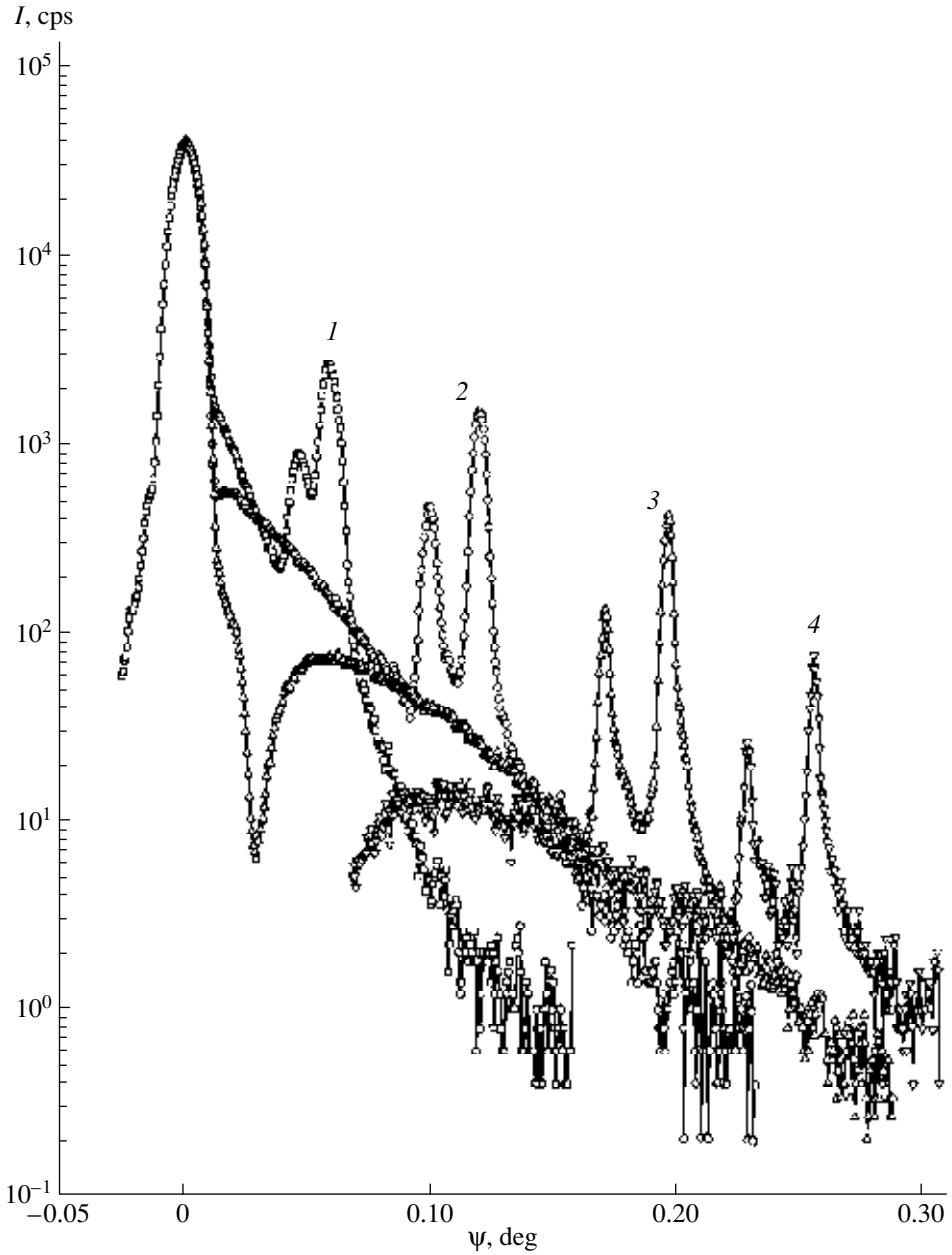

Fig. 4. Refraction patterns of diamonds at various glancing angles θ_1: (*1*) 0.60°, (*2*) 0.25°, (*3*) 0.09°, and (*4*) 0.01°.

$\theta_1/\mu(\lambda)$, and as θ_1 decreases, the intensity of the refracted beam decreases monotonically. The dependence is nonlinear, since the coefficient of reflection at the diamond–air interface tends to unity $R(\theta_1) \longrightarrow 1$ at $\theta_1 \longrightarrow 0$. The above regularities are confirmed by a series of refractograms obtained by angular scanning with detector *13* at several fixed grazing angles θ_1 (Fig. 4).

With going from the diamond to single-crystal silicon ($Z = 14$), the effective free path of x-ray photons $l_e = 1/\mu$ in the dispersive element decreases sharply for any wavelength in the spectral range considered. In particular, at $\lambda = 0.154$ nm (CuK_α line), we have μ(Si) = 145 cm^{-1} and μ(C) = 14.7 cm^{-1} [13–16]. According to Eq. (6), a decrease in $D(\rho, \lambda)$ should be observed for silicon in this case. As can be seen from Fig. 5, which displays the refractograms of Si (curve *1*) and C (curve *2*) for a grazing angle $\theta_1 = 0.08°$, the dispersive element made of silicon does not allow a complete resolution of the CuK_α and CuK_β spectral lines. At an acceleration voltage of 25 kV at the tube, the hardest part of the radiation spectrum in this case is not separated from the side wing of the primary beam that passes through the gap between the sample and shield *7* (Fig. 1).

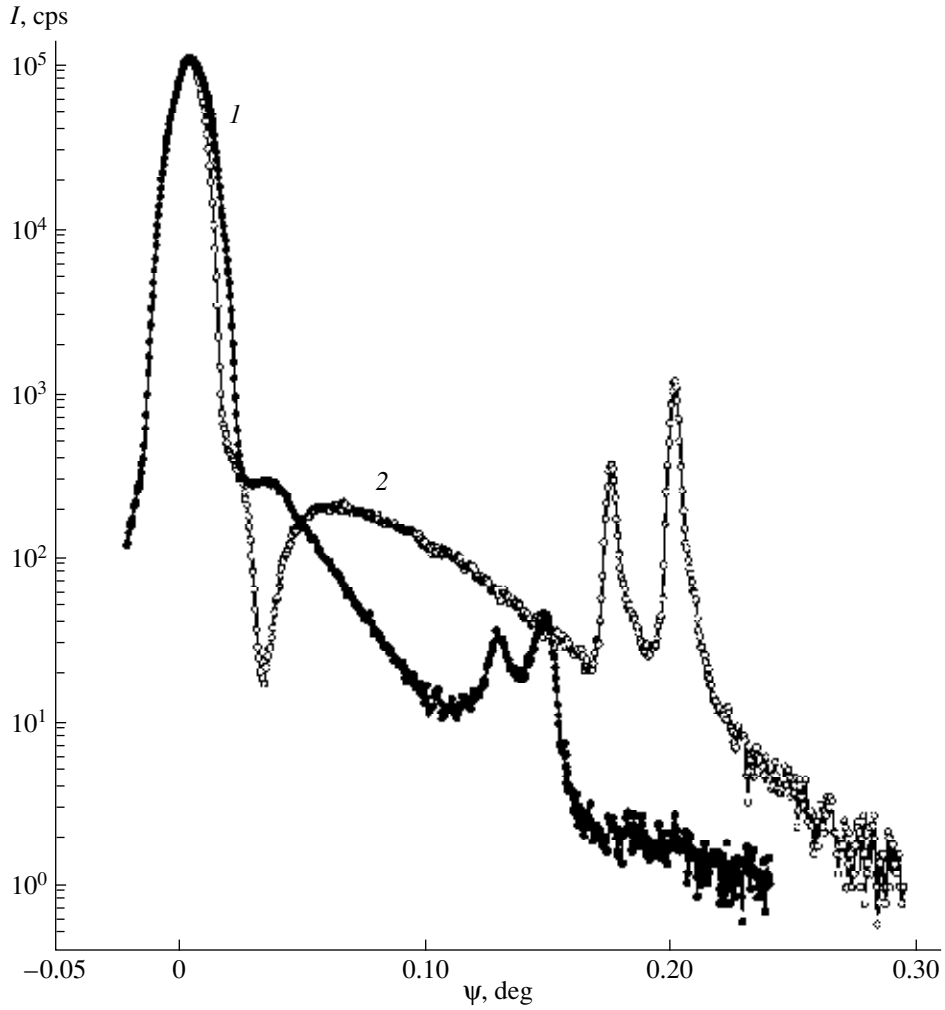

Fig. 5. Refraction patterns of (*1*) single-crystal silicon and (*2*) diamonds for a glancing angle $\theta_1 = 0.08°$ and a voltage at the x-ray tube $V = 25$ kV.

Figure 6 displays a series of refractograms of diamonds that were obtained at a fixed grazing angle $\theta_1 = 0.06°$ and various voltages at the x-ray tube in a range of 12 to 35 kV.

The spectral resolution of the diamond prism was determined using the refractogram (Fig. 7) that was obtained at $U_m = 40$ kV and $\theta_1 = 0.06°$. Measurements of the peak width at the half-height of the lines with the wavelengths of 0.154 and 0.139 nm with corrections for the instrumental function yield $\Delta\lambda = 19.7$ and 17.1 pm, respectively, or, on the energy scale, $\Delta E = 103$ and 110 eV, respectively. At smaller angles, as follows from Eq. (5), the spectral resolution should increase. No such an increase is observed in reality, since the radiation propagates along the surface through a distorted layer damaged by mechanical treatment, which increases the intensity of scattering by nonuniformities of the surface relief and leads to a smearing of the angular spectrum.

Thus, the investigations performed show the possibility of using a single-crystal diamond for practical measurements of hard x-ray radiation with wavelengths from 0.03 to 0.25 nm. This range includes the characteristic lines of the *K* and *L* series of virtually all elements with atomic numbers $Z > 25$. The range can be slightly extended to the long-wavelength region (to 0.3–0.5 nm) by fully or partially evacuating the working chamber in which the x-ray optical circuit is placed. With a further increase in λ, the absorption coefficient increases rapidly and the magnitude of *b* drops, which leads to a decrease in resolution due to diffraction effects related to the finite size of the effective refractive surface.

From the practical viewpoint, the most important result is that, owing to the angular dispersion of radiation, the full spectrum can be recorded using a single- or two-dimensional position detector, e.g., based on a linear or matrix CCD detector. This ensures the possi-

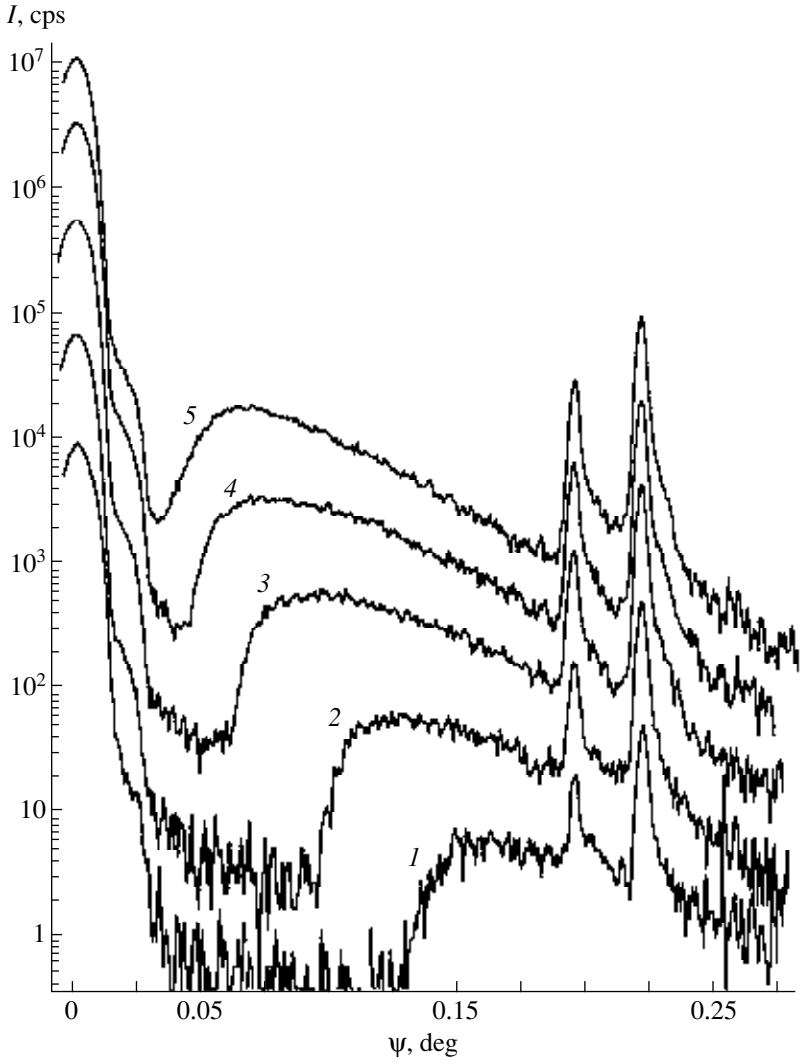

Fig. 6. Refraction patterns of a diamond at a glancing angle $\theta_1 = 0.06°$ and voltages at the x-ray tube equal to (*1*) 12, (*2*) 15, (*3*) 20, (*4*) 25, and (*5*) 35 kV.

bility of analyzing the spectrum without any restrictions on the magnitude of the time interval to be measured. Since the angular distribution is described well by Eq. (5) derived from the sine law and since the absorption properties of carbon have repeatedly been tabulated, we can calculate the spectral density of radiation $I^{\lambda}(\lambda)$ from the experimental dependence of $I(\varphi)$.

An alternative to diamonds as a material for dispersive elements is beryllium. In comparison with polycrystalline beryllium, the density of a natural diamond is greater by a factor of 1.9, which, according to Eq. (5), provides a higher angular dispersion. In addition, owing to the single-crystal structure, the scattering near the zero point of the reciprocal lattice is minimum. It is natural that, when using a polychromatic spectrum, some reciprocal-lattice points of single-crystal C (diamond) inevitably fall onto the Ewald sphere and part of energy flow will be dissipated into larger angles, in accordance with diffraction conditions. The diffraction scattering angles ϑ should be equal to or greater than $\geq \lambda/d$, where d is the maximum interplanar distance in the sample. In the spectral range under study, we have $\vartheta \gg \varphi$; i.e., the diffraction peaks cannot fall into the characteristic range of angles measured in refraction experiments. In addition, as was indicated above, the diffraction conditions are fulfilled only in narrow spectral bands for a finite set of reflections and, therefore, their presence virtually does not distort the monotonic distribution in the continuous part of the spectrum (Fig. 7). As to the characteristic lines, for a known crystallographic orientation of the diamond single crystal, we can always calculate in advance the angles between the refracting surface and atomic planes for which the

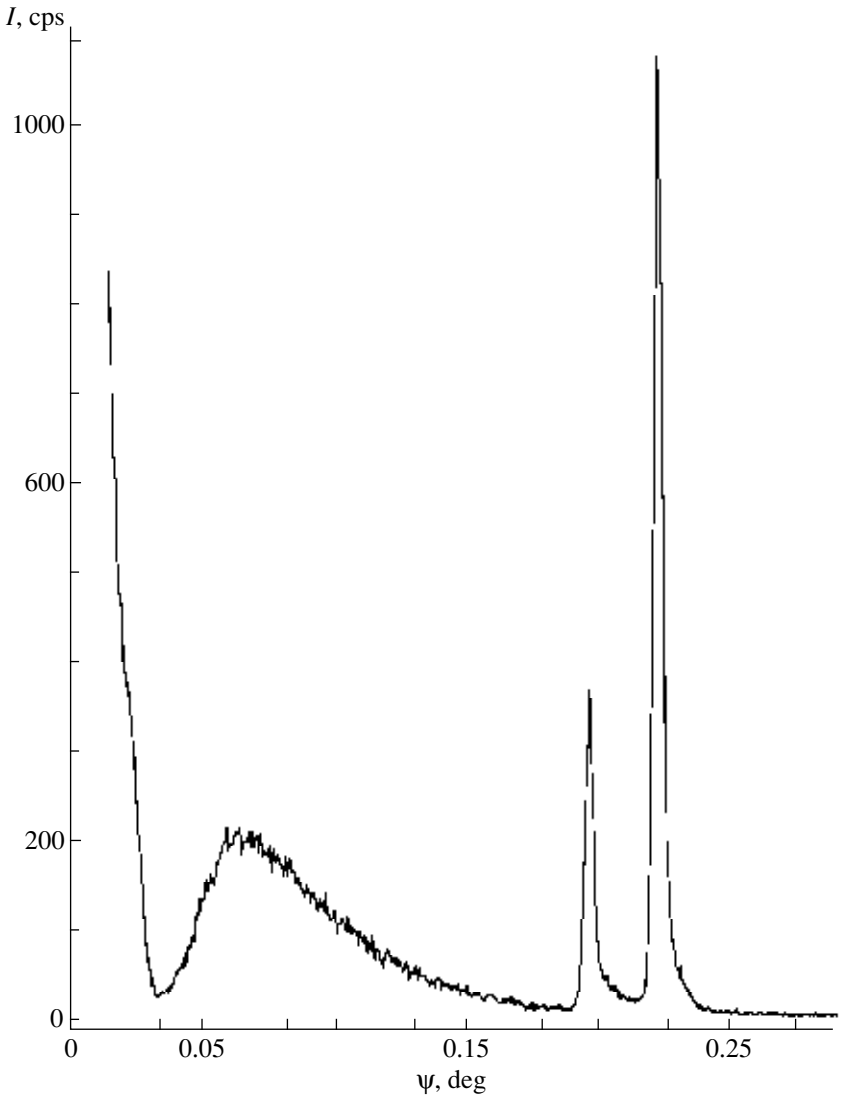

Fig. 7. Refraction pattern of a diamond at a glancing angle $\theta_1 = 0.06°$ and a voltage at the x-ray tube $V = 40$ kV.

diffraction conditions are not fulfilled for a given set of characteristic lines. Note that the samples of natural diamonds with an effective area of the refracting face of ~10 mm^2 that were used in our experiments are significantly cheaper than analogous synthetic crystals. In addition, in view of the mosaic structure of the latter, the spectral bands in which the intensity distribution in the angular spectrum can be distorted at the expense of Bragg reflections are wider in them than in natural crystals.

REFERENCES

1. *X-ray Techniques: A Handbook*, Ed. by V. V. Klyuev (Mashinostroenie, Moscow, 1980), Vol. 2, p. 60.
2. N. G. Volkov, V. A. Khristoforov, and N. P. Ushakov, in *Methods of Nuclear Spectrometry* (Énergoatomizdat, Moscow, 1990), p. 148.
3. J. A. Kyrala, J. Workman, S. Evans, *et al.*, in *Proceedings of the International Conference on High-Speed Photography and Photonics* (Moscow, 1998), p. 26.
4. K. N. Mukhin, in *Experimental Nuclear Physics* (Énergoatomizdat, Moscow, 1993), Vol. 1, Part 1.
5. L. S. Gorn and B. I. Khazanov, in *Modern Devices for Ionizing Radiation Measurements* (Énergoatomizdat, Moscow, 1989), p. 72.
6. R. Woldseth, *X-ray Energy Spectrometry* (Kevex Corporation, Burlingame, 1973; Atomizdat, Moscow, 1977).
7. A. Boscolo, L. Poletto, and G. Tondello, Pure Appl. Opt. **6** (1), L1 (1997).

8. A. V. Vinogradov, I. A. Brytov, A. Ya. Grudskiĭ, I. V. Kozhevnikov, M. T. Kogan, and V. A. Slemzin, *Mirror X-ray Optics* (Mashinostroenie, Leningrad, 1989).
9. M. Born and E. Wolf, *Principles of Optics* (Pergamon, Oxford, 1969; Nauka, Moscow 1973).
10. M. A. Blokhin, *Physics of X-rays* (GITTL, Moscow, 1957).
11. A. N. Zaĭdel', G. V. Ostrovskaya, and Yu. I. Ostrovskiĭ, *Techniques and Practice of Spectroscopy* (Nauka, Moscow, 1976).
12. A. G. Tour'yanskiĭ and I. V. Pirshin, Prib. Tekh. Éksp., No. 6, 104 (1999).
13. M. A. Blokhin and I. G. Shveĭtser, *A Handbook of X-ray Spectroscopy* (Nauka, Moscow, 1982).
14. B. L. Henke, E. M. Gullikson, and J. C. Davis, At. Data Nucl. Data Tables **54** (2), 181 (1993).
15. *Physical Quantities. Handbook*, Ed. by I. S. Grigor'ev and E. Z. Meĭlikhov (Énergoatomizdat, Moscow, 1991).
16. D. V. Fedoseev, N. V. Novikov, A. S. Vishnevskiĭ, and I. G. Teremetskaya, *Diamond: A Handbook* (Naukova Dumka, Kiev, 1981).

Translated by S. Gorin